THE JOURNAL OF PHYSICAL CHEMISTRY B

Article

pubs.acs.org/JPCB

Organogels from Dimeric Bile Acid Esters: In Situ Formation of Gold Nanoparticles

Arkajyoti Chakrabarty and Uday Maitra*

Department of Organic Chemistry, Indian Institute of Science, Bangalore 560012, Karnataka

Supporting Information

ABSTRACT: A new class of steroid dimers (bile acid derivatives) linked through ester functionalities were synthesized, which gelled various aromatic solvents. The organogels formed by the three dimeric ester molecules showed birefringent textures and fibrous nature by polarizing optical microscopy and scanning electron microscopy, respectively. A detailed rheological study was performed to estimate the mechanical strengths of two sets of organogels. In these systems, the storage modulus varied in the range of 0.8−3.5 × 10^4 at 1% w/v of the organogelators. The exponents of scaling of the storage modulus and yield stress of the two systems agreed well with those expected for viscoelastic soft colloidal gels with fibrillar flocs. The nanofibers in the organogel were utilized to engineer gold nanoparticles of different sizes and shapes and generate new gel−nanoparticle hybrid materials.

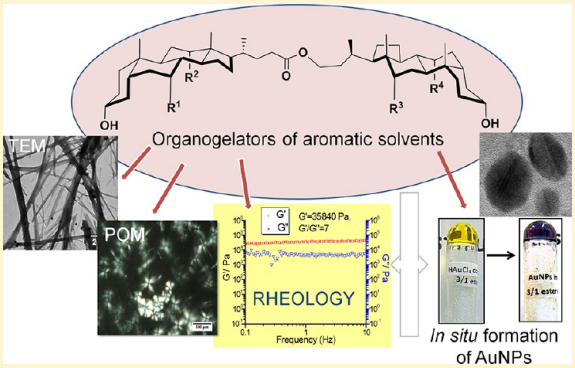

1. INTRODUCTION

During the last 2 decades, there has been a rapid growth in research on supramolecular organogels because of their potential applications.[1−8] An organogel is typically formed by the entrapment of solvent molecules by the entangled three-dimensional self-assembled fibrillar networks (SAFINs) formed from low molecular mass organogelators. The supramolecular association results from weak noncovalent interactions such as H-bonding, $\pi-\pi$ stacking, van der Waals, donor−acceptor interactions, and so forth. The formation of such an organogel is a thermoreversible process as the "gel" can be melted to a "sol" by heating above a characteristic gel melting temperature (T_g). The gel to sol transition can also happen reversibly (or irreversibly) in the presence of external physical or chemical stimuli (light, pH, etc.).[9−11] Several attempts have been made to correlate properties of the gels and the structures of the gelators.[12,13] Nevertheless, it is still not possible to a priori design a molecule that will selectively gelate a specific solvent. Thus, the discovery of organogelators results more from serendipity than from design.[1−6]

Bile acids/salts are physiologically important detergents, biosynthesized from cholesterol in the liver and stored in the gall bladder, and they help in digestion of fats in the small intestine.[14,15] Bile acids belong to the coprostane family of steroids and have the concave α-face with multiple hydroxyl groups, which make it hydrophilic, whereas the convex β-face (hydrocarbon-like) is hydrophobic. This facial amphiphilicity drives the self-aggregation of bile acids and their derivatives to form micelles and other supramolecular networks.[16,17] The organogelation property of bile acid derivatives arises mainly due to van der Waals and intermolecular hydrogen-bonding interactions involving the hydroxyl groups. There are only limited reports on bile-acid-based organogelators.[18−23] Our group has recently reported an acid/base-sensitive super-organogel of a bile derivative.[24]

Our group also reported organogel formation from simple esters of cholic acids.[18] This suggested that dimers and small oligomers of bile acids may also act as organogelators. In this work, we synthesized nine possible dimeric esters, and out of these, we discovered that three bile-acid-derived dimeric esters (**1**, **2**, and **3**) gelled aromatic solvents (Chart 1 and Figure 1). The organogels were characterized by polarizing optical microscopy, electron microscopy, and dynamic rheology. Finally, the nanostructures present in the **3**/1,2-dichlorobenzene (DCB) organogel were exploited as templates to synthesize gold nanoparticles (AuNPs) of different sizes and shapes. These gel−nanoparticle (NP) hybrid materials are efficient systems for applications in the field of biosensors, chiral catalysts, nonlinear optics, and material science.[25−27]

2. EXPERIMENTAL DETAILS

2.1. Materials. Lithocholic and 7-deoxycholic acids were supplied by Sigma and Fluka, respectively. 1,8-Diazabicyclo[5.4.0]undec-7-ene (DBU) was purchased from Sigma-Aldrich. All solvents were distilled prior to use. For AuNP synthesis, $HAuCl_4 \cdot 3H_2O$, sodium cyanoborohydride, and tetraoctylammonium bromide were purchased from Sigma-Aldrich.

Received: March 26, 2013
Revised: June 4, 2013

   dx.doi.org/10.1021/jp4029497 | J. Phys. Chem. B XXXX, XXX, XXX−XXX

Chart 1. Bile-Acid-Derived Dimeric Ester Organogelators (1−3)[a]

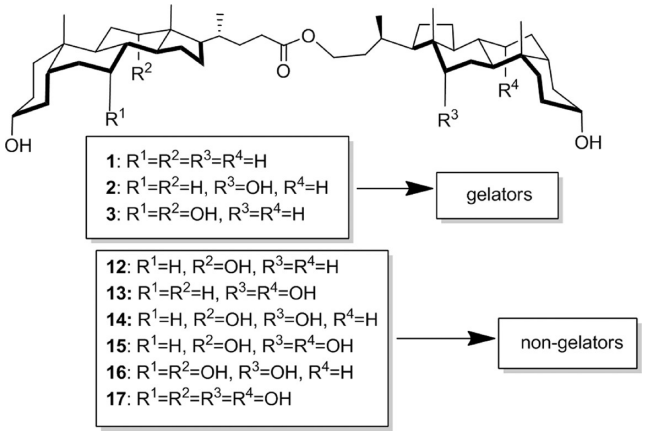

[a]The six dimers (**12**−**17**, non-gelators) are described in the Supporting Information.

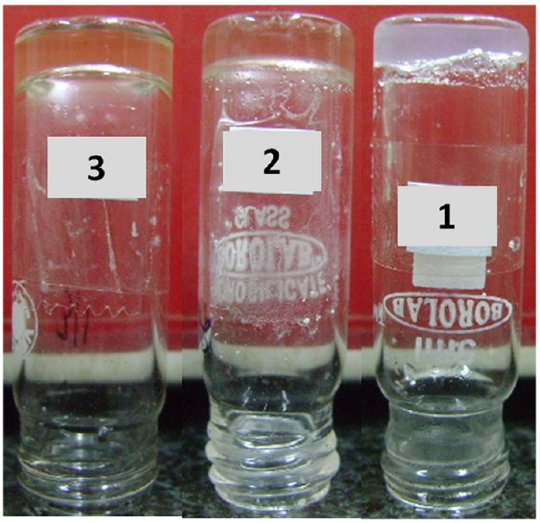

Figure 1. Photographs of the bile-acid-based dimeric ester organogels in 1,2-dichlorobenzene (from left to right): **3**, **2**, and **1** dimeric esters.

2.2. Synthetic Procedure. Organogelators **1**, **2**, and **3** were synthesized starting from lithocholic acid and 7-deoxycholic acid, as shown in Scheme 1. The syntheses of formylated lithocholic acid, deoxycholic acid, formyliodolithocholane, diformyliododeoxycholane were carried out according to a reported procedure.[28,29]

2.2.1. Compound 1. 3α-Hydroxy-5β-23-iodo-24-norcholane (0.18 g, 0.40 mmol) was dissolved in DMF (2 mL). Lithocholic acid (0.14 g, 0.36 mmol) was added followed by the addition of DBU (0.1 mL, 0.67 mmol). The solution was stirred at 55 °C for 24 h. After removing the volatiles, the crude product was purified by column chromatography using silica gel (1.2 cm × 12 cm) with 6−20% ethyl acetate/chloroform as the eluent to yield 0.18 g (64%) of the pure product. mp: 114−115 °C. $[\alpha]_D^{22}$: +40 (c. 2.0, EtOH). IR (KBr, cm^{-1}): 3347, 2937, 2865, 1736. ^{1}H NMR ($CDCl_3$, 400 MHz): δ 4.16−4.01 (m, 2H), 3.63 (m, 2H), 2.37−2.16 (m, 2H), 0.96−0.90 (12H), 0.65−0.64 (s, 6H). ^{13}C ($CDCl_3$, 100 MHz): δ 174.4, 71.8, 62.6, 56.5, 56.2, 56.0, 42.7, 42.1, 40.4, 40.1, 36.4, 35.8, 35.3, 34.6, 33.2, 31.4, 31.0, 30.5, 28.2, 27.2, 26.4, 24.2, 23.3, 20.8, 18.7, 18.2, 11.98. HRESI-MS (m/z): Calcd. for $C_{47}H_{78}O_4Na^+$ $[M+Na]^+$: 729.5798. Found: 729.5795. Anal. Calcd. for $C_{47}H_{78}O_4$: C, 79.83; H, 11.12. Found: C, 79.44; H, 10.82.

Scheme 1. Synthesis of the Gelators[a]

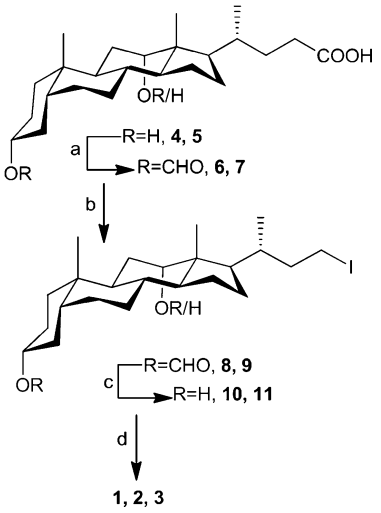

[a]Reaction conditions: (a) HCOOH, 55 °C, 5 h, 80−90%; (b) $Pb(OAc)_4/I_2/CCl_4/h\nu$/4 h, 60−70%; (c) K_2CO_3/MeOH/THF/2 h, rt, 90%; (d) lithocholic acid or cholic acid/DBU/DMF/55 °C/24 h; 64, 76, and 52%, respectively, for **1**, **2**, and **3**.

2.2.2. Compound 2. 3α,12α-Dihydroxy-5β-23-iodo-24-norcholane (0.2 g, 0.43 mmol) was dissolved in DMF (2 mL). Lithocholic acid (0.15 g, 0.39 mmol) was added followed by the addition of DBU (0.1 mL, 0.67 mmol). The solution was stirred at 55 °C for 24 h. After removing the volatiles, the crude product was purified by silica gel column chromatography (2 × 15 cm) and eluted with 2−6% EtOH−$CHCl_3$ as the eluent to yield 0.22 g (76%) of the pure product. mp: 135−136 °C. $[\alpha]_D^{22}$: +47 (c. 2.0, EtOH). IR (KBr, cm^{-1}): 3410, 2937, 2865, 1735, 1721. ^{1}H NMR ($CDCl_3$, 400 MHz): δ 4.14−4.04 (m, 2H), 3.99 (bs, 1H), 3.63 (m, 2H), 2.34−2.20 (m, 2H), 1.01−0.92 (12H), 0.69 (s, 3H), 0.64 (s, 3H). ^{13}C ($CDCl_3$, 100 MHz): δ 174.5, 73.1, 71.8, 62.6, 56.5, 55.9, 48.2, 47.6, 46.5, 42.7, 42.1, 40.4, 40.2, 36.4, 35.99, 35.8, 35.3, 34.5, 34.1, 33.6, 32.98, 31.3, 31.0, 30.5, 28.6, 28.2, 27.6, 27.1, 26.4, 26.1, 24.2, 23.6, 23.3, 23.1, 20.8, 18.2, 17.8, 12.6, 12.0. HRESI-MS (m/z): Calcd. for $C_{47}H_{78}O_5Na^+$ $[M+Na]^+$: 745.5747. Found: 745.5740. Anal. Calcd. for $C_{47}H_{78}O_5{\cdot}H_2O$: C, 76.17; H, 10.88. Found: C, 76.18; H, 10.47.

2.2.3. Compound 3. 3α-Hydroxy-5β-23-iodo-24-norcholane (0.2 g, 0.44 mmol) was dissolved in DMF (2 mL). Cholic acid (0.19 g, 0.46 mmol) was added followed by the addition of DBU (0.1 mL, 0.67 mmol). The solution was stirred at 55 °C for 24 h. After removing the volatiles, the crude product was purified by silica gel column chromatography (1.8 × 16 cm) with 6% EtOH−$CHCl_3$ as the eluent to yield 0.17 g (52%) of the pure product. mp: 107−110 °C. $[\alpha]_D^{22}$: +39 (c. 2.0, EtOH). IR (KBr, cm^{-1}): 3302, 2931, 2864, 1725, 755. ^{1}H NMR ($CDCl_3$, 300 MHz): δ 4.13−4.03 (m, 2H), 3.98 (bs, 1H), 3.85 (bs, 1H), 3.62 (m, 1H), 3.44 (m, 1H), 2.37−2.19 (m, 2H), 1.00−0.89 (12H), 0.68 (s, 3H), 0.65 (s, 3H). ^{13}C ($CDCl_3$, 75 MHz): δ 174.4, 73.0, 71.8, 68.4, 62.4, 56.5, 56.1, 47.1, 46.4, 42.77, 42.74, 42.1, 41.63, 41.60, 41.5, 40.47, 40.15, 39.5, 39.48, 36.34, 35.8, 35.3, 34.7, 34.5, 33.3, 31.6, 31.1, 30.5, 28.3, 27.2, 26.4, 24.2, 23.3, 22.4, 20.8, 18.7, 17.4, 12.5, 11.9. HRESI-MS (m/z): Cacld. for $C_{47}H_{78}O_6Na^+$ $[M+Na]^+$: 761.5696. Found:

dx.doi.org/10.1021/jp4029497 | J. Phys. Chem. B XXXX, XXX, XXX−XXX

761.5695. Anal. Calcd. for $C_{47}H_{78}O_6 \cdot 0.5H_2O$: C, 75.46; H, 10.64. Found: C, 75.32; H, 10.18.

2.3. Physical Measurements. Compounds **1**−**3** were screened at 1−3% w/v of the gelator by dissolving the gelators in a suitable solvent upon slight warming (at 60 °C) or at room temperature. For studies, test tubes containing the gels were sealed at the top, and the inverted test tubes were immersed in a paraffin oil bath and heated at a controlled rate (~2 °C/min) in a Heidolph stirrer-heater. The temperatures at which the gels fell under gravity were noted as the gel melting temperatures (T_g). For polarizing optical microscopic studies, a small piece of gel was scooped up and placed on a microscopic glass slide. A thin coverslip was put over the wet gel, and the sample was viewed under an Olympus BX 51 polarizing optical microscope. For scanning electron microscopic imaging, the gels were scooped up and placed on carbon tapes over aluminum stubs and dried under vacuum (10^{-3} Torr). The scanning electron microscopic images were recorded with FEI Sirion under an accelerating voltage of 10−15 keV with a 10 nm thick gold coating of the sample. For transmission electron microscopy (TEM) of the gel−NP hybrid materials, a Technai F30 machine was used. For UV−vis measurements, a Perkin-Elmer Lambda-35 absorption spectrometer was used.

2.4. Synthesis of AuNPs in an Organogel of 3 in DCB. $HAuCl_4 \cdot 3H_2O$ was dissolved in water (5 mL of 5 mM) and transferred to the 1,2-dichlorobenzene phase (5 mL) with the help of tetraoctylammonium bromide (2 mg). A yellow-colored 1,2-dichlorobenzene layer was obtained, indicating the presence of Au(III). Gelator **3** (5 mg, 6.76 μmol) was dissolved in 1,2-DCB containing Au(III) (0.4 mL) by heating at 60 °C for 30−40 s and sonicated for 20−30 s to obtain a transparent yellow gel. A solution of tetraoctylammonium borohydride was prepared by stirring sodium borohydride (5 mg) with tetraoctylammonium bromide (2 mg) in 1,2-DCB (4 mL). An aliquot of 0.2 mL of this reducing agent was added on the top of the gel and allowed to diffuse slowly into the gel. After a day, a purple/blue-colored gel was obtained. The gel was investigated by TEM and absorption spectroscopy. For preparing a sample for TEM, a carbon-coated copper grid was brought in contact with the gel to make a fine layer of the gel, and the sample was dried subsequently.

3. RESULTS AND DISCUSSION

3.1. Gelation Behavior. Compounds **1** and **3** formed strong gels in DCB (1% w/v). Dimer **3** was soluble in DCB at room temperature and formed a gel after keeping the solution at room temperature for 25−30 min. However, compound **1** has more versatile gelation properties as it gelled a wide variety of aromatic solvents, namely, toluene, mesitylene, benzene, and iodo-, bromo, and chlorobenzenes. Compound **2** was found to form a gel only in DCB, which formed slowly and was mechanically weak. However, at higher concentration (>2% w/v), it was possible to get mechanically stronger gels in DCB. With compounds **1** and **2**, the solid gelator was dissolved in the solvent by heating at 60 °C and kept at room temperature for gel formation. The gelation behavior of the three compounds is summarized in Table 1.

Table 1. Gelation Behavior of Bile-Acid-Derived Dimeric Ester Organogelators[a]

solvents	1	2	3
1,2-dichlorobenzene	G	TG	TG
chlorobenzene	G	P	TG
benzene	G	P	P
toluene	TG	P	P
mesitylene	G	P	P
xylene	G	P	P
iodobenzene	G	P	P
bromobenzene	G	P	P
fluorobenzene	G	P	P

[a]G: transparent gel; TG: translucent gel; P: precipitate.

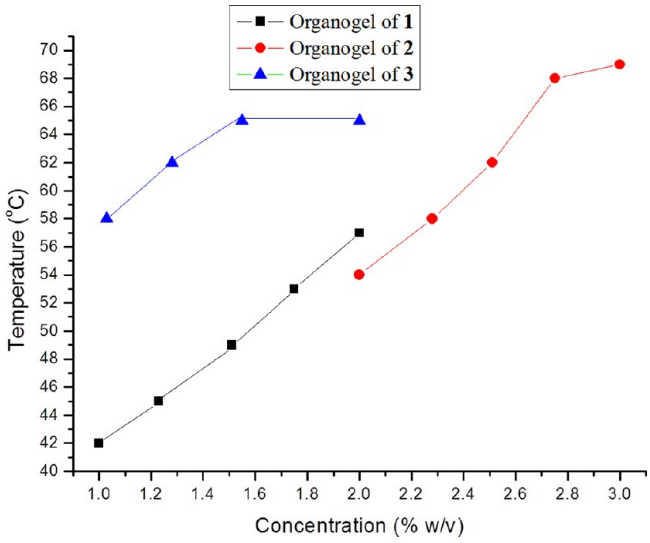

Figure 2. Gel melting temperatures of the organogels made with (a) **1**, (b) **2**, and (c) **3** in 1,2-dichlorobenzene.

3.2. Thermal Stability of the Gels. The thermal stability of the organogels of **1**−**3** were checked in 1,2-dichlorobenzene by the "inverted test tube method".[30] Dimer **3** showed higher thermal stability than dimer **1** in the same concentration range (1−2% w/v). Because dimer **2** formed less mechanically stable organogels at the concentration range of 1−2%, the concentration of the gelator was increased to 2−3% w/v for checking the gel melting temperatures.

The T_g versus concentration plots shown in Figure 2 indicate that for the same concentration range, the thermal stabilities were **3** > **1** > **2**.

3.3. POM and SEM Characterization of the Organogels. The wet gels of the three dimers in 1,2-dichlorobenzene were investigated by polarizing optical microscopy. The **1**-derived organogel in DCB showed birefringent patches suggesting anisotropic aggregation of the fibers in the entire three-dimensional network (Figure 3a). These birefringent patches showed different colors when a 530 nm filter was inserted into the path of the plane-polarized light coming out of the specimen. On the other hand, the **2**/DCB gel showed the presence of spherulite structures, commonly observed in liquid-crystalline gels (Figure 3b).[31,32] The presence of fibrous structures and birefringent patches was also featured in **3**/DCB organogel (Figure 3c).

The direct evidence of the three-dimensional microscopic organization of the gels was obtained from scanning electron microscopy. Flat tape like morphology of the network of the juxtaposed fibers was observed for **1**/DCB (Figure 4a). The **2**/DCB organogel showed fine fibrous three-dimensional networks. The fiber diameters were 40−80 nm, and they were highly entangled (Figure 4b). The self-assembled network of

dx.doi.org/10.1021/jp4029497 | J. Phys. Chem. B XXXX, XXX, XXX−XXX

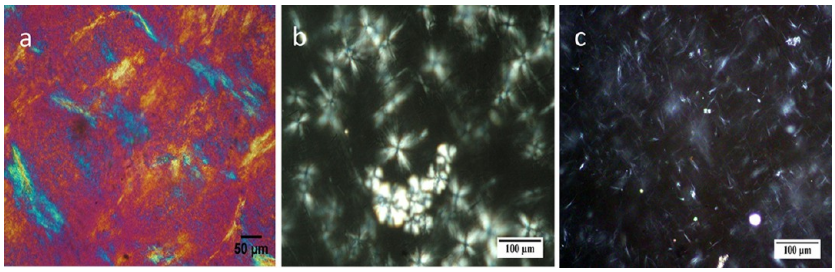

Figure 3. POM images of (a) **1**, (b) **2**, and (c) **3** dimeric ester organogels in DCB.

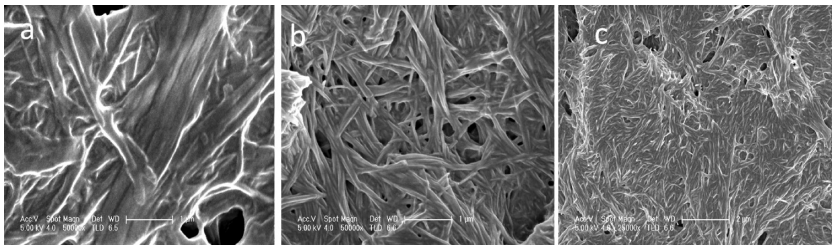

Figure 4. Scanning electron microscopic images of dimeric ester organogelators: (a) **1**-, (b) **2**-, and (c) **3**-derived xerogels in 1,2-dichlorobenzene.

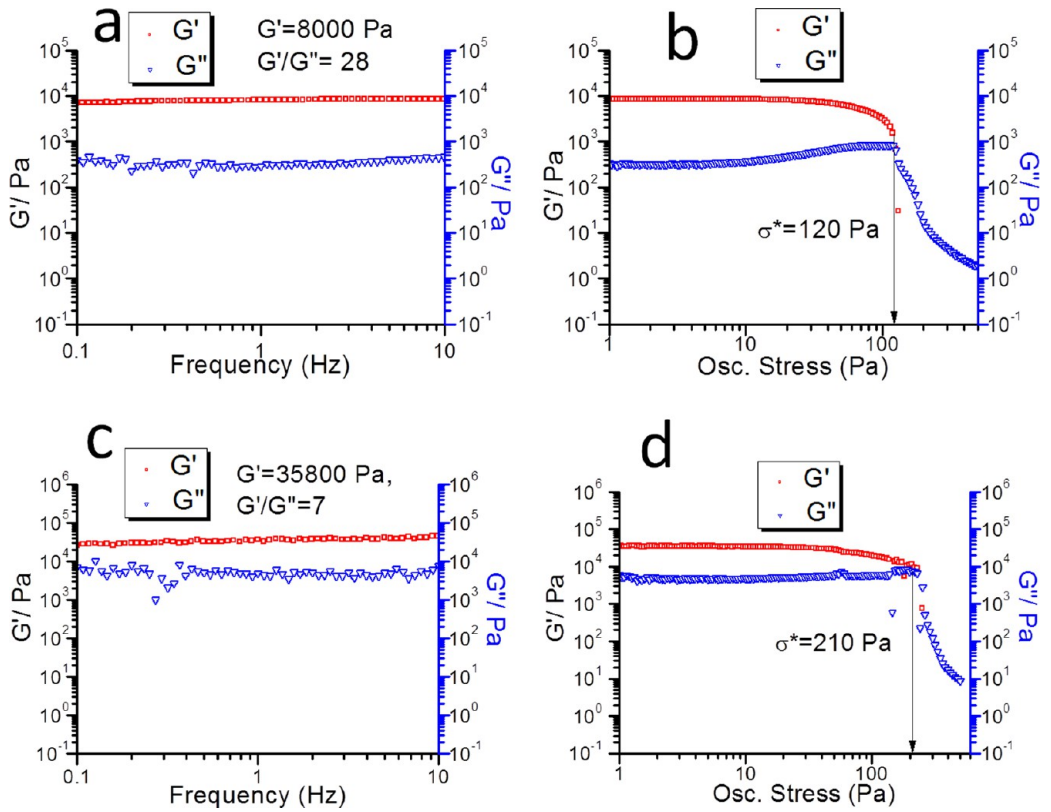

Figure 5. Dynamic rheological studies with the dimeric ester organogels: (a) frequency sweep and (b) stress sweep experiments of **1**/DCB organogel (1% w/v); and (c) frequency sweep and (d) stress sweep experiment of the **3**/DCB organogel (1% w/v). The frequency sweep test was performed at a fixed oscillatory stress of 1 Pa, and the values of G' and G'/G'' are calculated at f = 1 Hz. The σ^* values are obtained from a stress sweep test performed at a fixed frequency of 1 Hz.

Table 2. Rheological Parameters of 1 and 3 Organogels in 1,2-Dichlorobenzene (1% w/v)

system	solvent	G'/Pa	G'/G''	σ^*/Pa
1	DCB	8000	28	120
3	DCB	35800	7	210

the xerogel of **3** in DCB was made from 40−70 nm diameter fibers that were highly entangled and woven in a 3D network (Figure 4c).

3.4. Rheological Behavior of 1 and 3/DCB Organogels.

Gels are viscoelastic materials, and they both store as well as dissipate energy.[31,33] To understand the mechanical properties of the organogels, dynamic rheological experiments were

dx.doi.org/10.1021/jp4029497 | J. Phys. Chem. B XXXX, XXX, XXX−XXX

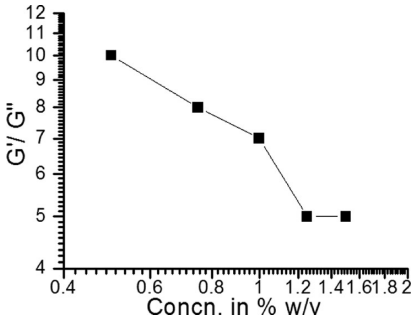

Figure 6. Plot of stiffness (G'/G'') versus concentration (% w/v) of the **3**/DCB organogel.

performed with the DCB gels of **1** and **3**. In oscillatory experiments, the viscoelastic behavior of the gels is characterized by the storage (G') and the loss (G'') moduli. Two types of experiments were performed with the organogels, (i) a frequency sweep test at a fixed oscillatory stress of 1 Pa and (ii) a stress sweep test at a fixed frequency of 1 Hz. The two important parameters that we get to know from the frequency sweep test are the dynamic storage modulus (G') and the stiffness defined by the ratio of G' to G'', whereas the stress sweep test reveals the critical oscillatory stress value at which the solid-like gel starts to flow due to the breakage of its three-dimensional network.

A comparative study of the DCB organogels of **1** and **3** organogels showed that at 1% w/v, compound **3** formed gels of higher mechanical strength than that of the compound **1** (G' of the **3**/DCB gel was almost 4 times that of **1**/DCB gel; Figure 5). The rheological data are shown in Table 2 and illustrate that while the **3**/DCB gel is stronger and more resistant to flow than the **1**/DCB gel, it is considerably less stiff.

The mechanical behavior shown by the two organogels qualify them as gels, and they can be compared with other low molecular mass organogels such as bisurea/cyclohexane and 12-hydroxystearic acid/nitrobenzene gels showing G' on the order of ~40 000 Pa.[34,35] To envisage the strength of the three-dimensional network present in the **3**/DCB organogel, we studied the variation of storage moduli, stiffness, and yield stress values of this gel at five different concentrations of the gelator, 0.5, 0.75, 1, 1.25, and 1.5% w/v.

The variation of the ratio (G'/G'') with the concentration of the gelator gives an idea of the amount of the stiffness in the gel. The gel exhibited a fall in the stiffness value as the concentration of the gelator was increased. Stiffness values of 8−10 at low concentration of the gelator (0.5−0.75) are common for viscoelastic soft solids, whereas a low value of

Table 3. Rheological Data of 3/DCB Organogel

concn (% w/v)	G'/Pa	G'/G''	σ^*/Pa	m of $G' = kC^m$	n of $\sigma^* = kC^n$
1	35800	7	210	2.91	2.75

Table 4. Parameters of the Theoretical Model of Strong-Link Regime: Colloidal Gels Containing Floc-like Elements

compound	m^a	n^a	d_f^b ($x = 1$)^c
3	2.91	2.75	1.63

[a] m and n are power exponents of the scaling of the storage modulus and the yield stress with concentration, respectively. [b] d_f is the fractal dimension of strongly interacting fibrillar flocs. [c] $x = 1$ is the fractal dimension of the skeleton of the fibrillar flocs.

stiffness, 5−7, at a higher concentration of the gelator indicates that the dissipation of energy through a viscous mechanism is more predominant in this concentration regime (Figure 6). Existence of variable balance of fiber association mechanisms (bundle formations, average mesh size, mean diameter, etc.) at different concentration regimes of the same gelator signifies this kind of behavior in the gels.[31]

However, the dependence of the elastic modulus and the yield stress on the concentration of the gelator can be obtained from the scaling laws, G' versus C^m or σ^* versus C^n (Figure 7). The scaling exponents dictate the way that a representative unit (i.e., floc or cell) in a gel is transduced through the macroscopic structure. There were noticeable increases in the storage modulus (G') and the yield stress (σ^*) with the concentration of the gelator, showing power law dependence in both cases (see Supporting Information Figure S1). The power law exponents were estimated from the slopes of the linear fits of the log−log plots of the storage modulus and yield stress versus concentration (C in % w/v) of the gelator (Figure 7a and b), and the values of the exponents are shown in Table 3. The exponents (m and n) were estimated to be ~2.9 and 2.7, respectively.

To analyze the above rheological data as mentioned in Table 3, we can consider the following theoretical model. To account for the typical behavior of elasticity (G') with the concentration of the gelator, the gel can be considered as colloidal-containing floc-like elements.[36,37] Depending on the strength of the inter- and intrafloc links, two regimes are possible, weak-link and strong-link regimes. The strong-link regime can be defined as the regime where interfloc links are stronger than the intrafloc links and the elasticity of the intrafloc links leads to the resulting elasticity of the gel. In the strong-link regime, the power exponent of storage modulus (m) can be deduced from eq 1

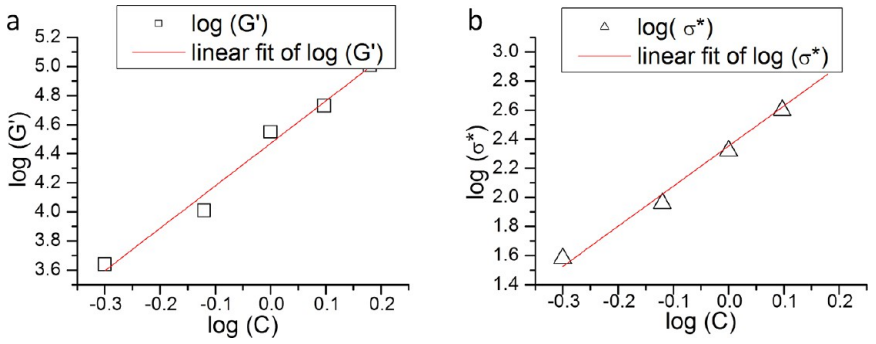

Figure 7. (a) Log−log plots of (a) the storage modulus (G') versus gelator concentration and (d) yield stress (σ^*) versus gelator concentration.

dx.doi.org/10.1021/jp4029497 | J. Phys. Chem. B XXXX, XXX, XXX−XXX

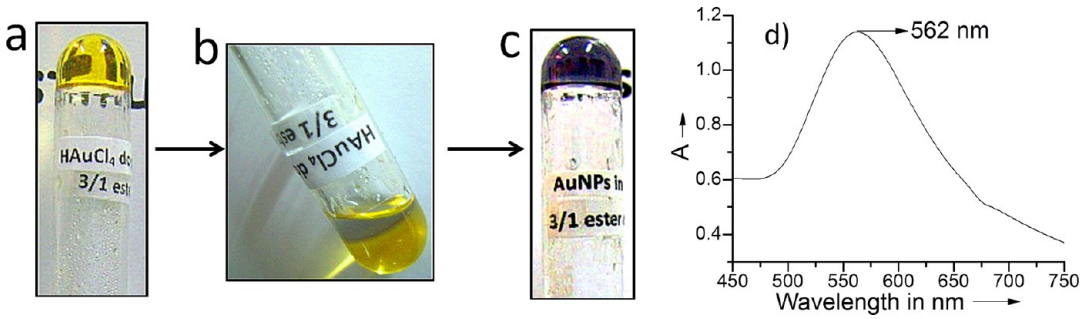

Figure 8. (a–c) Preparation of AuNPs embedded in **3**/DCB organogel fibers; (d) SPR band observed in the hybrid gel.

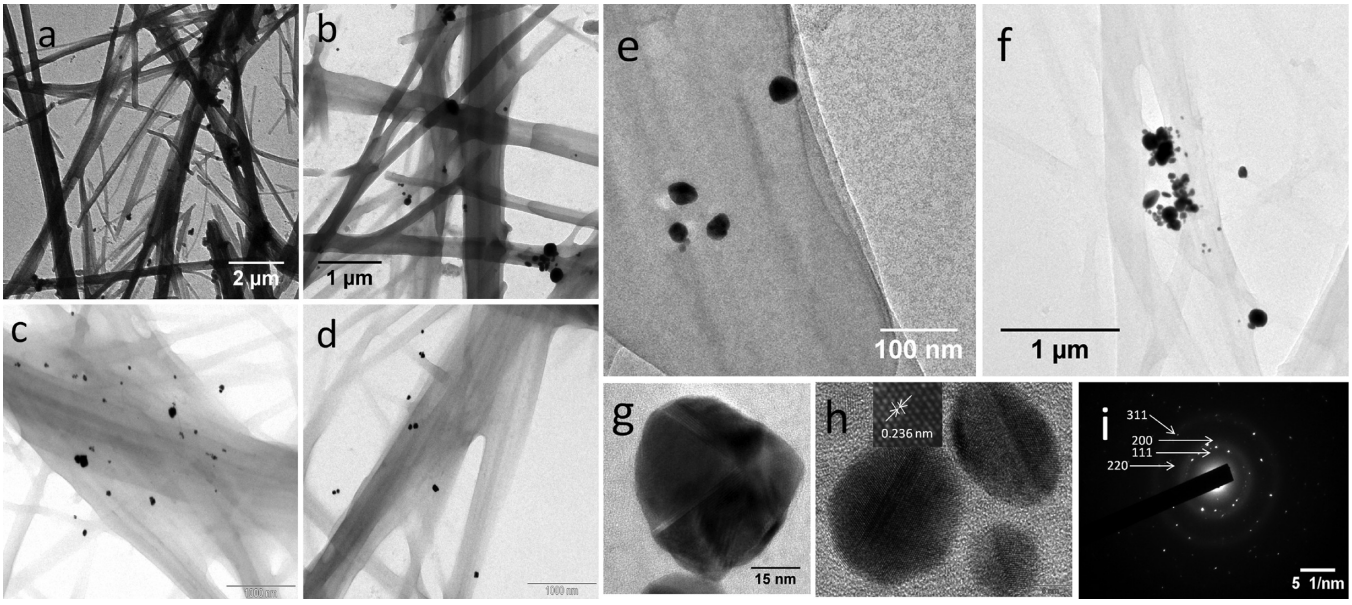

Figure 9. (a) The fibrillar network in the AuNP/organogel hybrid material (scale bar: 2 μm); (b–f) formation of gold nanocrystals of different shapes inside of the fibers (scale bars: 1 μm, 1 μm, 1 μm, 100 nm, and 1 μm, respectively), showing different regions of the same sample; (g,h) HRTEM images of the AuNPs formed inside of the fiber (scale bars: 15 and 5 nm, respectively; inset (h) lattice fringes); (i) SAED pattern showing single crystallinity of AuNPs.

$$m = \frac{(d + x)}{(d - d_f)} \quad (1)$$

where d is the Euclidean dimension of the system, d_f is the fractal dimension of the floc, and x is the fractal dimension of the backbone forming the floc. If we consider the strong-link regime as the possible model for the **3**/DCB organogel system, then $m = 2.91$ when $d_f = 1.63$ (assuming $x = 1$ for fibers). Thus, in the strong-link regime, the elasticity of the floc is controlled by a linear chain of springs, and that leads to the observation of the fractal dimension (d_f) = 1.6 for the **3**/DCB dimeric organogels. The strong-link regime is consistent with the visual observation of mechanically strong gels upon shaking for compound **3**. The values of the parameters are shown in Table 4.

3.5. Engineering of AuNPs in the Organogel Fibers from 3/DCB. Hybrid materials have become a burgeoning field in research because of their controlled and tunable electronic and optical properties, and they find use in lasers, waveguides, sensors, optoelectronics, and other smart systems.[38−44] Among the various metal NP−gel NP hybrid nanomaterials reported, AuNP−gel nanocomposites attract considerable attention due to the ease of synthesis of gold nanocrystals and potential application in catalysis, optics, and SERS.[42−44] Although there are various ways that one can fabricate NPs in the gel fibers,[45,46] we chose to design an in situ synthesis[47,48] of gold nanocrystals on the fibers of **3**/DCB organogel. Our idea was to first prepare the organogel in the desired solvent containing a gold precursor so that the gel fibers would contain a sufficient amount of Au(III) (Figure 8a). In the next step, a reducing agent such as tetrabutylammonium borohydride (see the Experimental Details section) was added at the top of the gel layer to reduce Au(III) to Au(I) (Figure 8b). In this fashion, a purple/blue-colored gel−NP hybrid material can be obtained (Figure 8c). The surface plasmon resonance band was at 562 nm, indicating the presence of large nanocrystals in the sample (Figure 8d).[49−52]

TEM indeed showed the presence of gold nanocrystals of average particle size of 30 nm diameter embedded in the fibers of the organogel (Figure 9).

Upon generation of AuNPs, the gel fibers could sustain their nanostructures (Figure 9a) and thus provide a framework to stabilize the NPs. However, there were few nanocrystals with larger diameter (~100−120 nm) accumulated in the "junction zones" of the fibrillar network (Figure 9b). The shapes of the nanocrystals were varied; tetrahedral, ellipsoidal, and spherical structures of AuNPs were observed in the gel fibers (Figure 9b−h). The distance of the lattice fringes was determined to be

dx.doi.org/10.1021/jp4029497 | J. Phys. Chem. B XXXX, XXX, XXX−XXX

0.236 nm in the HRTEM image of the gold nanocrystals (Figure 9h, inset), and the selected area electron diffraction (SAED) pattern of the AuNPs synthesized in this fashion exhibits bright diffraction spots characteristic of larger crystal grains possessing single crystallinity.[53,54] The SAED pattern can further be indexed according to (111), (200), (220), and (311) reflections of the fcc structure of Au (Figure 9i).

Thus, the strategy used to synthesize AuNPs in situ in the gel fibers was successful and presents a useful way of accessing gold nanocrystals of different shapes and sizes (~20−40 nm). The anisotropic faces of the nanocrystals have different surface atom densities, electronic structures, and chemical reactivities[53] and thus can be further exploited.[55−58]

4. SUMMARY AND CONCLUSIONS

In conclusion, among nine dimeric steroids synthesized, three bile acid dimers were shown to possess the organogelation property. From the structural point of view, the lithocholane/lithocholic acid part plays a major role in driving the organogelation (cf. other dimers/nongelators in the Supporting Information), as reported previously from our group.[24] Polarizing microscopy of the organogels revealed liquid-crystalline textures present in the wet gels, whereas scanning electron microscopic images of the xerogels showed the highly entangled and fine fibrous morphology (thin 40−80 nm diameter fibers) present in these gels. In terms of rheological behavior, the **3**/DCB organogel was found to be mechanically stronger than that of the **1**/DCB organogel. The storage modulus and the yield stress were found to increase proportionately with the concentration of the gelator **3** and showed power law dependence. To apply the dimeric ester organogels as functional materials, a new strategy was adopted to fabricate the gold nanocrystals inside of the gel fibers in situ, and the gel network plays an essential role of stabilizing the AuNPs. Our future target is to explore the hybrid materials in advanced applications.

■ ASSOCIATED CONTENT

Ⓢ Supporting Information

Synthesis and characterization of other bile-acid-based dimeric esters (nongelators), copies of NMR spectra, and some additional rheological data of the **3**/DCB organogel. This material is available free of charge via the Internet at http://pubs.acs.org.

■ AUTHOR INFORMATION

Corresponding Author

*E-mail: maitra@orgchem.iisc.ernet.in.

Notes

The authors declare no competing financial interest.

■ ACKNOWLEDGMENTS

The Department of Science & Technology is thanked for the award of the JC Bose Fellowship to U.M. and for support of this work through Grant No. SR/S1/OC-68/2011. A.C. thanks CSIR for a research fellowship.

■ REFERENCES

(1) Terech, P.; Weiss, R. G. Low Molecular Mass Gelators of Organic Liquids and the Properties of Their Gels. *Chem. Rev.* **1997**, *97*, 3133−3160.

(2) Abdallah, D. J.; Weiss, R. G. Organogels and Low Molecular Mass Organic Gelators. *Adv. Mater.* **2000**, *12*, 1237−1247.

(3) van Esch, J. H.; Feringa, B. L. New Functional Materials Based on Self-Assembling Organogels: From Serendipity towards Design. *Angew. Chem., Int. Ed.* **2000**, *39*, 2263−2266.

(4) Fages, F. Metal Coordination to Assist Molecular Gelation. *Angew. Chem., Int. Ed.* **2006**, *45*, 1680−1682.

(5) John, G.; Jadhav, S. R.; Menon, V. M.; John, V. T. Flexible Optics: Recent Developments in Molecular Gels. *Angew. Chem., Int. Ed.* **2012**, *51*, 1760−1762.

(6) Babu, S. S.; Prasanthkumar, S.; Ajayaghosh, A. Self-Assembled Gelators for Organic Electronics. *Angew. Chem., Int. Ed.* **2012**, *51*, 1766−1776.

(7) Ren, Y.; Kan, W. H.; Thangadurai, V.; Baumgartner, T. Bio-Inspired Phosphole-Lipids: From Highly Fluorescent Organogels to Mechanically Responsive FRET. *Angew. Chem., Int. Ed.* **2012**, *51*, 3964−3968.

(8) Banerjee, S.; Das, R. K.; Maitra, U. Supramolecular Gels 'In Action'. *J. Mater. Chem.* **2009**, *19*, 6649−6687.

(9) Murata, K.; Aoki, M.; Nishi, T.; Ikeda, A.; Shinkai, S. New Cholesterol-Based Gelators with Light- and Metal-Responsive Functions. *J. Chem. Soc., Chem. Commun.* **1991**, 1715−1718.

(10) Ayabe, M.; Kishida, T.; Fujita, N.; Sada, K.; Shinkai, S. Binary Organogelators Which Show Light and Temperature Responsiveness. *Org. Biomol. Chem.* **2003**, *1*, 2744−2747.

(11) Pozzo, J. L.; Clavier, G. M.; Desvergne, J.-P. Rational Design of New Acid-Sensitive Organogelators. *J. Mater. Chem.* **1998**, *8*, 2575−2577.

(12) Lin, Y.-C.; Kacher, B.; Weiss, R. G. Liquid-Crystalline Solvents as Mechanistic Probes. Part 37. Novel Family of Gelators of Organic Fluids and the Structure of Their Gels. *J. Am. Chem. Soc.* **1989**, *111*, 5542−5551.

(13) Garner, C. M.; Terech, P.; Allegrand, J.-J.; Mistrot, B.; Nguyen, P.; Geyer, A. D.; Rivera, D. Thermoreversible Gelation of Organic Liquids by Arylcyclohexanol Derivatives Synthesis and Characterization of the Gels. *J. Chem. Soc., Faraday Trans.* **1998**, *94*, 2173−2179.

(14) *The Bile Acids Chemistry, Physiology and Metabolism*; Nair, P. P., Kritchevsky, D., Eds.; Plenum Press: New York, 1973; Vol. *2*.

(15) *Steroids and Bile Acids*; Danielson, H., Sjovall, J., Eds.; Elsvier: Amsterdam, The Netherlands, 1985.

(16) Mukhopadhyay, S.; Maitra, U. Chemistry and Biology of Bile Acids. *Curr. Sci.* **2004**, *87*, 1666−1683.

(17) Weiss, R. G.; Terech, P. *Molecular Gels: Materials with Self-Assembled Fibrillar Networks*; Springer: New York, 2006.

(18) Nonappa; Maitra, U. Simple Esters of Cholic Acid as Potent Organogelators: Direct Imaging of the Collapse of SAFINs. *Soft Matter* **2007**, *3*, 1428−1433.

(19) Hishikawa, Y.; Sada, K.; Watanabe, R.; Miyata, M.; Hanabusa, K. A Novel Class of Organogelator Based on N-Isopropycholamide and the First Observation of Fibrous Colloidal Aggregates. *Chem. Lett.* **1998**, *27*, 795−796.

(20) Nakano, K.; Hishikawa, Y.; Sada, K.; Miyata, M.; Hanabusa, K. Novel Gelators of Bile Acid-Alkylamine Salt Prepared through a Combinatorial Library Approach. *Chem. Lett.* **2000**, *29*, 1170−1171.

(21) Willemen, H. M.; Vermonden, T.; Marcelis, A. T. M.; Sudhölter, E. J. R. N-Cholyl Amino Acid Alkyl Esters — A Novel Class of Organogelators. *Eur. J. Org. Chem.* **2001**, 2329−2335.

(22) Willemen, H. M.; Vermonden, T.; Marcelis, A. T. M.; Sudhölter, E. J. R. Alkyl Derivatives of Cholic Acid as Organogelators: One-Component and Two-Component Gels. *Langmuir* **2002**, *18*, 7102−7106.

(23) Willemen, H. M.; Marcelis, A. T. M.; Sudhölter, E. J. R.; Bowman, W. G.; Demé, B.; Terech, P. A Small-Angle Neutron Scattering Study of Cholic Acid-Based Organogel Systems. *Langmuir* **2004**, *20*, 2075−2080.

(24) Maitra, U.; Chakrabarty, A. Protonation and Deprotonation Induced Organo/hydrogelation: Bile Acid Derived Gelators Containing a Basic Side Chain. *Beilstein J. Org. Chem.* **2011**, *7*, 304−309.

(25) Braun, P. V.; Osenar, P.; Stupp, S. I. Semiconducting Superlattices Templated by Molecular Assemblies. *Nature* **1996**, *380*, 325−328.
(26) Jung, J. H.; Ono, Y.; Hanabusa, K.; Shinkai, S. Creation of Both Right-Handed and Left-Handed Silica Structures by Sol−Gel Transcription of Organogel Fibers Comprised of Chiral Diaminocyclohexane Derivatives. *J. Am. Chem. Soc.* **2000**, *122*, 5008−5009.
(27) Shone, E. D.; Zubarev, E. R.; Stupp, S. I. Semiconductor Nanohelices Templated by Supramolecular Ribbons. *Angew. Chem., Int. Ed.* **2002**, *41*, 1705−1709.
(28) Bhat, S.; Maitra, U. Low Moecular Mass Cationic Gelators Derived from Deoxycholic Acid: Remarkable Gelation of Aqueous Solvents. *Tetrahedron* **2007**, *63*, 7309−7320.
(29) Babu, P.; Maitra, U. Synthesis and In Vitro Cholesterol Dissolution by 23- and 24- Phosphonobile Acids. *Steroids* **2005**, *70*, 681−689.
(30) Clavier, G. M.; Brugger, J.-F.; Bouas-Laurent, H.; Pozzo, J.-L. 2,3-Di-n-alkoxyanthraquinones as Gelators of Organic Solvents. *J. Chem. Soc., Perkin Trans. 2* **1998**, 2527−2534.
(31) Sangeetha, N. M.; Bhat, S.; Choudhury, A. R.; Maitra, U.; Terech, P. Properties of Hydrogels Derived from Cationic Analogues of Bile Acid: Remarkably Distinct Flowing Characteristics. *J. Phys. Chem. B* **2004**, *108*, 16056−16063.
(32) Huang, X.; Terech, P.; Raghavan, S. R.; Weiss, R. G. Kinetics of 5α-Cholestan-3β-yl-*N*-(2-Naphthyl)carbamate/*n*-Alkane Organogel Formation and Its Influence on the Fibrillar Networks. *J. Am. Chem. Soc.* **2005**, *127*, 4336−4344.
(33) Terech, P.; Sangeetha, N. M.; Maitra, U. Molecular Hydrogels from Bile Acid Analogues with Neutral Side Chains: Network Architectures and Viscoelastic Properties. Junction Zones, Spherulites, and Crystallites: Phenomenological Aspects of the Gel Metastability. *J. Phys. Chem. B* **2006**, *110*, 15224−15233.
(34) Brinksma, J.; Feringa, B. L.; Kellogg, R. M.; Vreekar, R.; van Esch, J. H. Rheology and Thermotropic Properties of Bis-Urea-Based Organogels in Various Primary Alcohols. *Langmuir* **2000**, *16*, 9249−9255.
(35) Terech, P.; Pasquier, D.; Bordas, V.; Rossat, C. Rheological Properties and Structural Correlations in Molecular Organogels. *Langmuir* **2000**, *16*, 4485−4494.
(36) Wu, H.; Morbidelli, M. A Model Relating Structure of Colloidal Gels to Their Elastic Properties. *Langmuir* **2001**, *17*, 1030−1036.
(37) Shi, W.-H; Shi, W. Y.; Kim, S.-I; Liu, J.; Aksay, I. A. Scaling Behavior of the Elastic Properties of Colloidal Gels. *Phys. Rev. A* **1990**, *42*, 4772−4779.
(38) Simmons, B.; Li, S.; John, V. T.; Mc Pherson, G. L.; Taylor, C.; Schwartz, D. K.; Maskos, K. Spatial Compartmentalization of Nanoparticles into Strands of a Self-Assembled Organogel. *Nano Lett.* **2002**, *2*, 1037−1042.
(39) Kimura, M.; Kobayashi, S.; Kuroda, T.; Hanabusa, K.; Shirai, H. Assembly of Gold Nanoparticles into Fibrous Aggregates Using Thiol-Terminated Gelators. *Adv. Mater.* **2004**, *16*, 335−338.
(40) Love, C. S.; Chechik, V.; Smith, D. K.; Wilson, K.; Ashworth, I.; Brennan, C. Synthesis of Gold Nanoparticles within a Supramolecular Gel-Phase Network. *Chem. Commun.* **2005**, 1971−1973.
(41) Ray, S.; Das, A. K.; Banerjee, A. Smart Oligopeptide Gels: In Situ Formation and Stabilization of Gold and Silver Nanoparticles within Supramolecular Organogel Networks. *Chem. Commun.* **2006**, 2816−2818.
(42) Daniel, M.-C.; Astruc, D. Gold Nanoparticles: Assembly, Supramolecular Chemistry, Quantum-Size-Related Properties, and Applications toward Biology, Catalysis, and Nanotechnology. *Chem. Rev.* **2004**, *104*, 293−346.
(43) Mahmoudi, M.; Azadmanesh, K.; Shokrgozar, M. A.; Journeay, W. S.; Laurent, S. Effect of Nanoparticles on the Cell Life Cycle. *Chem. Rev.* **2011**, *111*, 3407−3432.
(44) Bhat, S.; Maitra, U. Nanoparticle−Gel Hybrid Material Designed with Bile Acid Analogues. *Chem. Mater.* **2006**, *18*, 4224−4226.
(45) Sangeetha, N. M.; Bhat, S.; Raffy, G.; Belin, C.; Loppient-Serani, A.; Aymonier, C.; Terech, P.; Maitra, U.; Desvergne, J.-P.; Guerzo, A. D. Hybrid Material Combining Photoactive 2,3-DidecyloxyAnthracene Physical Gels and Gold Nanoparticles. *Chem. Mater.* **2009**, *21*, 3424−3432.
(46) *Hybrid Materials, Synthesis, Characterization and Applications*; Kickelbick, G., Ed.; Wiley VCH: Weinheim, Germany, 2007.
(47) Chakrabarty, A.; Maitra, U.; Das, A. D. Metal Cholate Hydrogels: Versatile Supramolecular Systems for Nanoparticle Embedded Soft Hybrid Materials. *J. Mater. Chem.* **2012**, *22*, 18268−18274.
(48) At the time that we were preparing this manuscript, a work on in situ generation of gold and silver nanoparticles in the supramolecular hydrogel came out; see: Shen, J.-S.; Chen, Y.-L.; Huang, J.-L.; Chen, J.-D.; Zhao, C.; Zheng, Y.-Q.; Yu, T.; Yang, Y.; Zhang, H.-W. Supramolecular Hydrogels for Creating Gold and Silver Nanoparticles In Situ. *Soft Matter* **2013**, *9*, 2017−2023.
(49) Jin, R.; Egusa, S.; Scherer, N. F. Thermally-Induced Formation of Atomic Au clusters and Conversion into Nanocubes. *J. Am. Chem. Soc.* **2004**, *126*, 9900−9901.
(50) Kim, F.; Connor, S.; Song, H.; Kuykendall, T.; Yang, P. D. Platonic Gold Nanocrystals. *Angew. Chem., Int. Ed.* **2004**, *43*, 3673−3677.
(51) Sosa, I. O.; Noguez, C.; Barrera, R. G. Optical Properties of Metal Nanoparticles with Arbitrary Shapes. *J. Phys. Chem. B* **2003**, *107*, 6269−6275.
(52) Sun, X. P.; Dong, S. J.; Wang, E. K. Large-Scale Synthesis of Micrometer-Scale Single-Crystalline Au Plates of Nanometer Thickness by a Wet-Chemical Route. *Angew. Chem., Int. Ed.* **2004**, *43*, 6360−6363.
(53) Wang, Z. L. Transmission Electron Microscopy of Shape-Controlled Nanocrystals and Their Assemblies. *J. Phys. Chem. B* **2000**, *104*, 1153−1175.
(54) Huang, W.; Qian, W.; El-Sayed, M. A.; Ding, Y.; Wang, Z. L. Effect of the Lattice Crystallinity on the Electron−Phonon Relaxation Rates in Gold Nanoparticles. *J. Phys. Chem. C* **2007**, *111*, 10751−10757.
(55) Julián, B.; Corbeán, R.; Cordoncillo, E.; Escribano, P.; Viana, B.; Sanchez, C. Synthesis and Optical Properties of Eu^{3+}-Doped Inorganic−Organic Hybrid Materials Based on Siloxane Networks. *J. Mater. Chem.* **2004**, *14*, 3337−3343.
(56) Li, L.-L.; Yang, C.-J.; Chen, W.-H.; Lin, K.-J. Towards the Development of Electrical Conduction and Lithium-Ion Transport in a Tetragonal Porphyrin Wire. *Angew. Chem., Int. Ed.* **2003**, *42*, 1505−1508.
(57) Roquet, S.; Cravino, A.; Leriche, P.; Allevêque, O.; Frere, P.; Roncali, J. Triphenylamine−Thienylenevinylene Hybrid Systems with Internal Charge Transfer as Donor Materials for Heterojunction Solar Cells. *J. Am. Chem. Soc.* **2006**, *128*, 3459−3466.
(58) Sanchez, C.; Julian, B.; Belleville, P.; Popall, M. Applications of Hybrid Organic−Inorganic Nanocomposites. *J. Mater. Chem.* **2005**, *15*, 3559−3592.